Int J Thermophys (2014) 35:2215–2225
DOI 10.1007/s10765-014-1586-4

Cavity-Enhanced Absorption Spectroscopy and Photoacoustic Spectroscopy for Human Breath Analysis

J. Wojtas · F. K. Tittel · T. Stacewicz · Z. Bielecki · R. Lewicki · J. Mikolajczyk · M. Nowakowski · D. Szabra · P. Stefanski · J. Tarka

Received: 17 November 2013 / Accepted: 13 March 2014 / Published online: 1 April 2014

Abstract This paper describes two different optoelectronic detection techniques: cavity-enhanced absorption spectroscopy and photoacoustic spectroscopy. These techniques are designed to perform a sensitive analysis of trace gas species in exhaled human breath for medical applications. With such systems, the detection of pathogenic changes at the molecular level can be achieved. The presence of certain gases (biomarkers), at increased concentration levels, indicates numerous human diseases. Diagnosis of a disease in its early stage would significantly increase chances for effective therapy. Non-invasive, real-time measurements, and high sensitivity and selectivity, capable of minimum discomfort for patients, are the main advantages of human breath analysis. At present, monitoring of volatile biomarkers in breath is commonly useful for diagnostic screening, treatment for specific conditions, therapy monitoring, control of exogenous gases (such as bacterial and poisonous emissions), as well as for analysis of metabolic gases.

J. Wojtas (✉) · Z. Bielecki · J. Mikolajczyk · M. Nowakowski · D. Szabra
Institute of Optoelectronics, Military University of Technology, 2 Kaliskiego Str., 00-908 Warsaw, Poland
e-mail: jwojtas@wat.edu.pl

F. K. Tittel · R. Lewicki · P. Stefanski · J. Tarka
Electrical and Computer Engineering Department, Rice University, Houston, TX 77005, USA

T. Stacewicz
Institute of Experimental Physics, University of Warsaw, 69 Hoza Str., 00-681 Warsaw, Poland

R. Lewicki
Sentinel Photonics, 11 Deer Park Dr., STE 208, Monmouth Junction, NJ 08852, USA

P. Stefanski · J. Tarka
Laser and Fiber Electronics Group, Wroclaw University of Technology, 27 Wybrzeze Wyspianskiego Str., 50-370 Wroclaw, Poland

Keywords Absorption spectroscopy · Biomarker sensors · Cavity-enhanced spectroscopy · Gas sensors · Laser drivers · Laser spectroscopy · Photoacoustic spectroscopy

1 Introduction

An analysis of human breath is useful for health and wellness-state monitoring. The presence of specific gases (known as biomarkers) at elevated concentration levels in exhaled human breath indicates several human diseases. Their concentration depends on the individual characteristics of a person. For example, the concentration of exhaled nitric oxide varies with age, gender, lung capacity, and time of day. Moreover, smoking, alcohol consumption, air pollution, and physiological factors also have an impact on the exhaled air composition [1]. Typical biomarkers include: *carbon monoxide*—oxidation of fatty acids, *ammonia*—protein catabolism caused by ammonia and amino acids, *carbon disulfide*—intestinal bacteria, *hydrocarbons*—metabolism and lipid peroxidation, and *methanol*—due to metabolism of fruit [1–3]. Examples of biomarkers are listed in Table 1 [4]. According to the recommendations by the American Thoracic Society (ATS), high NO concentration levels >50 ppb for adult patients and >35 ppb for children can be caused by atopic asthma, eosinophilic bronchitis, or chronic obstructive pulmonary disease (COPD) with mixed inflammatory phenotype. The volatile biomarkers are analyzed using various techniques such as gas chromatography (GC), mass spectrometry (MS), or chemiluminescence [5]. Recently, there has been an increasing interest in developing and applying optoelectronic methods [6,7]. Laser spectroscopy is especially useful for trace gas detection. This approach provides the opportunity to detect (based on absorption) the presence of a target analyte. It is used for quantitative detection and monitoring of chemical trace gas species. The absorption is determined by measuring the radiation quenching when passing through the medium. The decrease in the intensity of radiation that is transmitted from a laser source is measured with a photodetector. Other approaches include the measurement of indirect absorption effects induced by radiation: temperature changes, photoacoustic

Table 1 Examples of disease biomarkers [4]

Breath gas	Formula	Typical fraction	Diseases
Carbon monoxide	CO	(0.01 to 10) ppm	Asthma, angina, hyperbilirubinemia
Ammonia	NH_3	0 to 2 ppm	Liver disease, stomach ulcers, and duodenal ulcers caused by helicobacter pylori
Nitric oxide	NO	(10 to 50) ppb	Asthma
Ethane	C_2H_6	0 to 10 ppb	Alzheimer disease, atherosclerosis, diabetes, cancer
Carbonyl sulfide	OCS	0 to 10 ppb	Liver disease, transplant rejection
Hydrogen cyanide	HCN	0 to 10 ppb	Cystic fibrosis

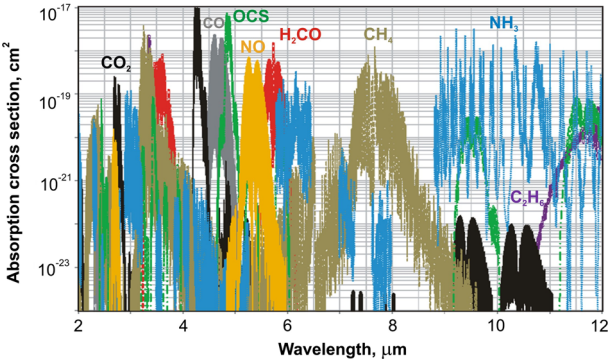

Fig. 1 Absorption spectral cross sections of selected biomarkers (based on the HITRAN database)

spectroscopy (PAS), and the measurement of electric current or charge in the medium (optogalvanic spectroscopy).

Absorption spectra of molecules result from quantum transitions that occur between molecular energy levels. In the ultraviolet spectral range (UV), these spectra are quasi-continuous and correspond to the transitions between electronic states. At normal operating conditions when collisional and Doppler broadening occur, the individual transitions between ro-vibrational levels are not distinguishable. Therefore, the selective detection of species is difficult in the UV. In the mid-infrared, the absorption bands correspond to transitions between molecular ro-vibrational levels of the ground electronic state [8]. These spectra predominately consist of narrow separated lines that provide the opportunity to selectively detect a diatomic and triatomic molecular trace gas species even in the presence of an interfering gas such as H_2O or CO_2 which might compound even 10 % of a breath. For effective trace gas detection, the appropriate selection and matching of sensor parameters to the absorption spectra of the investigated molecules is extremely important. The absorption cross sections as a function of wavelength for selected relevant biomedically trace gas species are depicted in Fig. 1.

The light sources that are useful in laser absorption spectroscopy (LAS) should be compact, capable of operating with high laser output power and stable single-mode operation (both in the cw or pulsed operating regime), and long lifetimes. Taking into account the above mentioned requirements, both gas and solid-state lasers might be effective [9,10]. These laser sources are characterized by good beam parameters and often offer high output power radiation. However, such lasers have disadvantages, e.g., require a complex power supply design, the necessity of efficient cooling (usually liquid), significant overall size, and high cost. Moreover, in many cases the production of tunable radiation requires additional technologies. The main ones are difference frequency generation (DFG) and optical parametric oscillation (OPO). These systems are characterized by complex design, associated with substantial cost and the requirement of stable operating conditions. The development of a compact OPO was reported in [11]. Both CW DFG- and OPO-based instruments provide narrow spectral bandwidth and output powers (up to tens of mW). Reference [12] reports the design and demonstration of a resonant OPO that provides a high output power.

An important milestone in the development of mid-IR LAS occurred in 1994 with the development of quantum cascade lasers (QCLs) [13,14]. QCLs are suitable for CEAS and PAS for human breath analysis because of their integrated design, narrow spectral linewidth, high output power (both cw and pulsed), and convenience of wavelength tuning by means of current and temperature control. Application of these lasers in spectroscopy provides an opportunity to design compact and cost effective mid-IR trace gas sensor systems. In this paper, a compact novel QCL module integrated with a complete laser current and temperature control system for different spectroscopy techniques is presented.

2 Experiments

2.1 Cavity-Enhanced Absorption Spectroscopy

Typical sensor systems employing simple spectrophotometry attain a detection limit up to $10^{-4}\,\mathrm{cm}^{-1}$ [4]. The CEAS-based sensors can provide a detection limit of $\sim 10^{-9}\,\mathrm{cm}^{-1}$. CEAS was proposed by Engeln et al. [15] in 1998 as a modification of cavity ring-down spectroscopy (CRDS). The basic operating concept of both methods is similar, i.e., in both techniques a high quality optical cavity is formed by two highly reflective concave mirrors as shown in Fig. 2. This results in a long effective optical path, reaching up to several kilometers. The difference between CEAS and CRDS is related to the alignment of a mid-IR laser beam into the cavity and the associated longitudinal and axial mode structures. In CEAS, radiation is injected at a very small angle with respect to the cavity axis. This results in the formation of a dense structure of weak longitudinal modes, which can overlap with each other. An effective modification of CEAS is the use of a piezoelectric-driven output mirror that modulates the cavity length which in turn results in a constant axial mode structure [16].

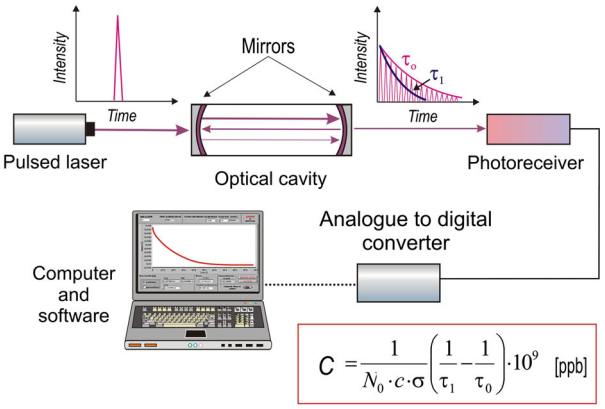

N_0 - Loschmidt number, τ_1 - decay time with absorber, τ_0 - decay time without absorber, c - light speed, σ - gas absorption cross section.

Fig. 2 Schematic of CEAS method

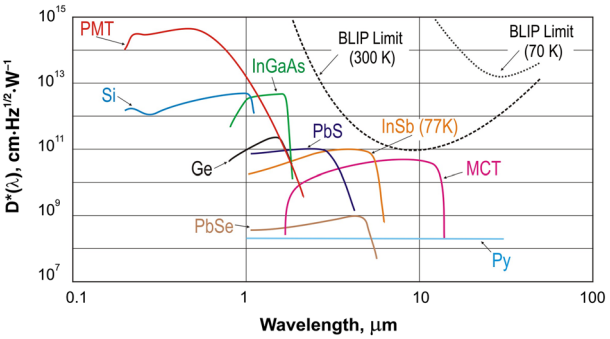

Fig. 3 Spectral detectivity of commercially available photodetectors as a function of wavelength

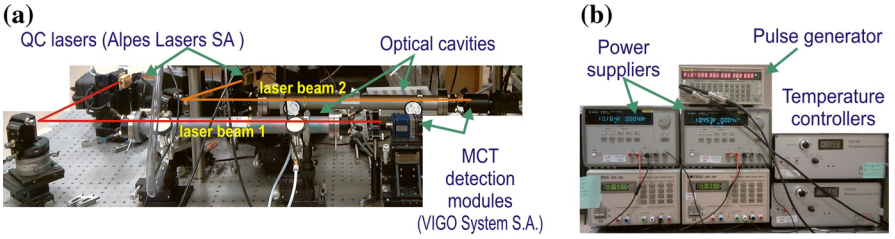

Fig. 4 CEAS (a) experimental setup and (b) control system for two QCLs

Furthermore, due to off-axis alignment, the interference by the feedback radiation from the cavity mirror is eliminated.

The optical signal from the cavity is detected by a mid-IR, low noise, and sensitive detector. The operating spectral response of the detector should be matched to the selected absorption line of the investigated trace gas species. In the ultraviolet (UV), visible (VIS), and near-infrared (NIR $< 1.7\,\mu$m) spectral ranges, the most common detectors are photomultiplier tubes (PMTs). PMTs are characterized by high gain, high speed, and low dark current [17–19]. For mid-IR radiation, InSb photodiodes, PbSe photoresistors, as well as MCT photoresistors and photodiodes are the optimum choices [20,21]. However, their detectivity and speed are lower than PMTs (Fig. 3). The ultimate mid-IR photodetector performance is attained when the density of photon-generated carriers in the detector is greater than the density of thermal carriers. For these conditions, the photodetector noise is dominated by fluctuations in the carriers generated by the incident background flux, known as background limited performance (BLIP).

Research conducted in the Institute of Optoelectronics at the Military University of Technology, and in the Institute of Experimental Physics at the University of Warsaw confirmed the high sensitivity of NO and NH_3 sensors based on the CEAS method (Fig. 4a). In both cases, a detection limit of $\sim$30 ppb was obtained. The detection limit was determined using a laboratory calibration system, which consisted of a modular gas standard generator 491M type (KIN-TEK Laboratories, Inc.). The 491M included a secondary dilution module (491M-SD), a gas feed module (491M-GF), and a humidified gas module (491M-HG). The generator was used to produce gas mixtures

Table 2 Parameters of selected QCLs

Laser type	Power (W)	Wavelength (μm)	Operation temperature (K)	Spectral tuning (cm^{-1})
DFB-QCL	2.4	4.8	RT	4.0
RCSE-QCL	0.4	4.9	RT	–
QCL array	1.1	9	RT	220
Multi-section QCL	0.08	9.3	RT	450
EC-QCL	0.035	3.2	RT	83
Optically tunable QCL	0.10	9.0	RT	0.3

containing NO and NH_3 trace concentrations. The detection limit was determined for the lowest concentration of the analyzed gas, which resulted in a measurable change of the output signal of the sensor.

The measurement procedure for a CEAS sensor consists of a two-step process. First, a measurement of the signal decay time (τ_0) for the optical cavity without the absorber (analyzed gas) is performed. Subsequently, the signal decay time τ for the cavity filled with the analyzed gas is carried out. Therefore, the uncertainty of time measurements limits the precision of such sensors. The decay time τ_0 depends on the length of the resonator and the mirror reflectivity. Therefore, the longer the decay time, the longer is the effective path of absorption and the lower is the concentration level of the absorber that can be measured [18]. During our experiments, an uncertainty of 10 % was obtained after 2 s integration time. The uncertainty decreases with increasing signal-to-noise ratio (SNR). Therefore, the implementation of a more powerful QCL (Table 2) and cavities with a higher Q-factor significantly improves detection limits that are possible.

Our control system for two QCLs is shown in Fig. 4b. It consists of a pulse generator, precise voltage sources, power suppliers for laser drivers, and temperature controllers. Recently, an analog control electronics unit (CEU) capable of driving the QCL current and temperature lock-in detection and wavelength scanning was developed in order to reduce the footprint of the overall sensor system architecture. Details of the CEU for QCLs are described in Sect. 2.3. There are several QCL design structures that are suitable for LAS, i.e., Fabry-Perot (FP-QCLs), distributed feedback (DFB-QCLs), and external cavity QCL designs (EC-QCLs) or lasers with integrated built-in difference frequency generation structure (DFG-QCLs) [22]. FP lasers are characterized by a multimode type of operation. Therefore, they generate higher optical power from the single structure (∼120 W). In contrast, single-mode operation and precise control of the emission wavelength are possible using a DFB-QCL. EC-QCLs with a broad spectral emission ($>500\,cm^{-1}$) are useful tools for spectroscopic trace gas measurements [23,24]. Such QCLs that simultaneously generate at several wavelengths within a large tuning range have been reported [25]. For example, a two-wavelength QCL emitting at both 5.2 μm and 8.0 μm or covering an ultrabroad band in the spectral range from 6.0 μm to 8.0 μm was first developed by Gmachl et al. [25]. Furthermore, DFB-QCL arrays have been designed. These structures provide spectral tuning of $\sim 200\,cm^{-1}$ with a linewidth (FWHM) of $\sim 0.01\,cm^{-1}$ and $\sim 0.0001\,cm^{-1}$ for pulsed or cw operation mode, respectively [9].

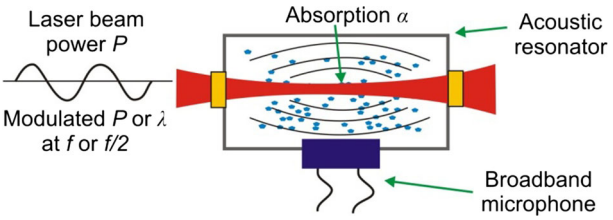

Fig. 5 Photoacoustic spectroscopy concept

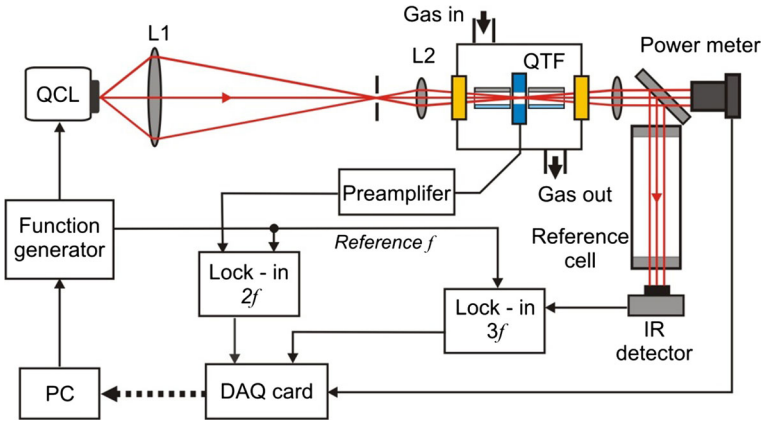

Fig. 6 Block diagram of quartz-enhanced photoacoustic spectroscopy (QEPAS)-based trace gas sensor system

2.2 Quartz-Enhanced Photoacoustic Spectroscopy (QEPAS)

Photoacoustic spectroscopy is based on conversion of modulated light energy into a sound wave in absorbing materials [26]. Traditionally, the photoacoustic signal is detected with a resonant acoustic cell equipped with a sensitive microphone (Fig. 5). QEPAS can be implemented by replacing the microphone used in PAS with a resonant quartz tuning fork (QTF) [27]. QEPAS-based sensor platforms are characterized by a simple design, immunity to environmental acoustic noise, applicability over a wide range of pressures, and the capability to analyze gas sample volumes as small as $\sim$1 cm^3 (Fig. 6).

QEPAS systems that use commercially available QTFs with a resonant frequency of $\sim$32.8 kHz and a Q-factor of 10^5 in vacuum and $\sim 10^4$ at 760 Torr have been reported [14]. Only the symmetric vibration of a QTF is piezoelectrically active. The excitation beam passes through the gap between the QTF prongs for efficient excitation of this vibration. The measurements are usually performed with wavelength modulation (WM) using $2f$ detection. The WM technique suppresses the background originating from spectrally non-selective absorbers (such as resonator walls, QTF electrodes, and gas cell elements). The QCL lasing wavelength should be matched to a selected absorption line of the targeted trace gas species, similar to CEAS. A lock-in amplifier is used to detect the QTF signal. In order to increase the effective

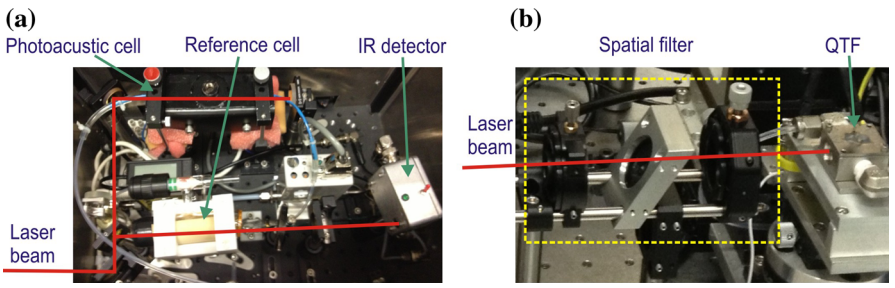

Fig. 7 Photos of two experimental sensor systems: (a) PAS and (b) QEPAS

interaction length between the radiation-induced sound and the QTF, a gas-filled acoustic microresonator can be applied similar to the traditional PAS approach. In addition for line locking purposes, a reference cell filled typically with a high concentration of the targeted gas and an IR detector (for, e.g., a low cost pyroelectric detector) are added to the system in order to register $1f$ or $3f$ signals. For example, QEPAS-based NO and NH_3 sensors provide the opportunity to construct ultra-compact systems with a detection limit of single or even sub-ppb [28].

The experiments at the Rice University Laser Science Group Laboratory showed that PAS and QEPAS sensor architectures are able to detect $\sim$3 ppb of NH_3 when targeting the 965.4 cm^{-1} NH_3 absorption line located in the υ_2 fundamental absorption band of ammonia. Measurements were performed with a widely tunable EC-QCL system (Daylight Solution) operated at a wavelength of about 10.5 μm. In the case of PAS (Fig. 7a), the laser beam was directed to the photoacoustic cell and to the reference cell. In order to improve the detection limit, the beam was passed through the photoacoustic cell three times. A mechanical chopper operating at 1.759 kHz (resonance frequency of the photoacoustic cell) was used for amplitude modulation of the laser radiation. In the QEPAS setup, the 9 cm long PAS cell was replaced with an approximately 1 cm long QTF detection module, placed after a spatial filter (Fig. 7b). Moreover, the modulation of laser current was performed by a low amplitude sinusoidal signal with a frequency matched to the half of the QTF resonance frequency ($\sim$16.4 kHz), according to the requirements of the $2f$ detection technique.

In Fig. 8, the influence of the gas pressure on the PAS signal is presented and, as expected, lower pressures result in narrower trace gas absorption lines. The reported data were normalized to the maximum value of the signal at 600 Torr. A measurement error of 0.3 % was reached after averaging the data over $>$5 min.

In PAS, the vibrational–translational relaxation rate of gas molecules plays an important role. The energy transfer from excited molecules by means of non-radiative processes is faster at higher pressures. This results in a higher acoustic excitation and greater absorption signal as a function of pressure. In the case of a slow relaxation rate with respect to the modulation frequency, the PAS signal decreases. This is due to the fact that the translational gas temperature cannot follow fast changes of the laser-induced molecular excitation rate. QEPAS measurements, which are performed at a detection frequency of 32.8 kHz, are more sensitive to the vibrational relaxation rate compared to the conventional PAS which is commonly performed at a frequency of

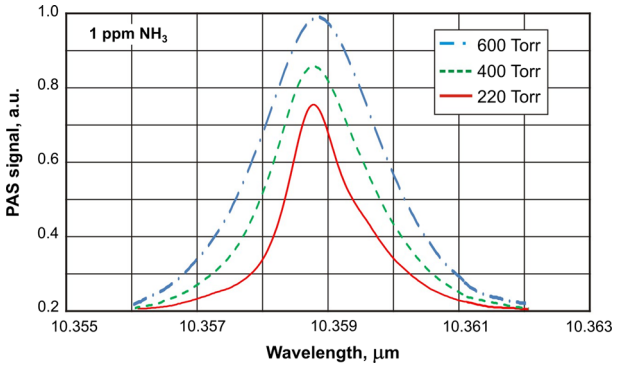

Fig. 8 Example of normalized PAS signals for 1 ppm NH_3 at four different pressure values

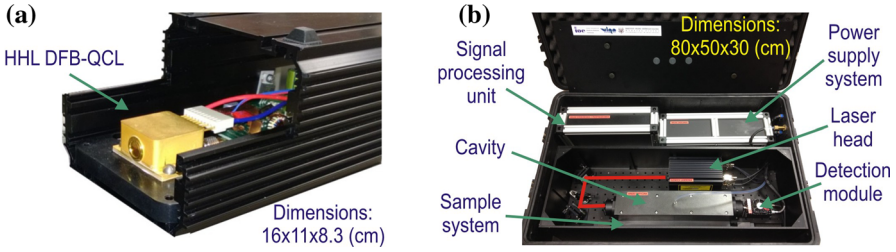

Fig. 9 Photos of (a) compact laser head and (b) its application as a portable NO sensor

1.759 kHz. The maximum QEPAS signal occurs at an optimum pressure that depends on the targeted molecular species and the QTF parameters. The presence of H_2O (usually RH $< 0.2\,\%$) can increase the relaxation rate of the target gas, and impact the measured QEPAS signal [28,29]. In our experiments, a humidifier made from thin Nafion tubes (Perma Pure LLC) was applied.

2.3 Portable Sensor Developing

After experiments using lab setups, a portable, ultra-sensitive sensor was developed for CEAS spectroscopy. The main device of the sensor is a compact laser head that consists of a laser mount and an enclosure. The device is capable of controlling signal levels that are delivered to the QCL from current and temperature drivers (Fig. 9a). In addition, there is also a cooling system that consists of a TEC controller and a water-cooled heat exchanger which helps to stabilize the temperature of the CW DBF-QCL mounted inside a high heat load (HHL)-type housing. The laser head also provides a current ramp that can be superimposed with a modulation signal (e.g., a series of short pulses or sinusoidal pulses). The sub-threshold ramp signal heats the QCL so that each QCL pulse is generated at a different wavelength. This technique is called inter-pulse modulation [30,31]. Such a design makes it possible to develop compact sensors employing PAS, QEPAS, and wavelength modulation spectroscopy (WMS). As an example, a compact NO sensor for use in the CEAS technique was constructed

as shown in Fig. 9b. It consists of a developed laser head supplied from batteries, and elements used during an experiment described in Sect. 2.1, i.e., a cavity, a simple gas sample system, a detection module (VIGO System), and a signal processing unit. In the laser head, a DFB-QCL with an operating laser wavelength of 5.26 μm from Alpes Lasers was used. During the experiments using a laboratory calibration system (see Sect. 2.1), this sensor achieved a NO minimum detection limit of 30 ppb at room temperature operating conditions (25 °C).

3 Conclusions

The described laser spectroscopy techniques are characterized by high sensitivity. CEAS is useful in the radiation spectral range where the most sensitive photodetectors (photomultipliers) are available (UV, VIS, NIR). Problems occur for longer wavelengths due to the relatively low photodetector detectivity. PAS or QEPAS techniques might offer a solution. However, in order to obtain high detection sensitivity results, a laser source of several tens of mW is required. Preliminary experiments showed that our sensor systems can be applied to nitric oxide (according to ATS recommendations) and ammonia detection as biomarkers of pathogenic changes. CEAS-, PAS-, and QEPAS-based trace gas sensors will be useful for health monitoring, because of real-time and non-invasive monitoring, ease to use, as well as minimum inconvenience for patients.

Acknowledgments These works were supported by the National Centre for Research and Development (research Project ID 179900) and the National Science Centre (research Project Nos. 2011/03/B/ST7/02544, ON515 216839, and ON515 217039).

References

1. L. Pauling, A.B. Robinson, R. Teranishi, P. Cary, Proc. Natl. Acad. Sci. USA **68**, 2374 (1971)
2. H. O'Neill, S.M. Gordon, M. O'Neill, R.D. Gibbons, J.P. Szidon, Clin. Chem. **34**, 1613 (1988)
3. C. Wang, P. Sahay, Sensors **9**, 8230 (2009). doi:10.3390/s91008230
4. J. Wojtas, Z. Bielecki, T. Stacewicz, J. Mikolajczyk, M. Nowakowski, Opto Electron. Rev. **201**, 77 (2012)
5. A. Ulanowska, T. Ligor, M. Michel, B. Buszewski, Ecol. Chem. Eng. S **17**, 9 (2010)
6. B. Buszewski, D. Grzywinski, T. Ligor, T. Stacewicz, Z. Bielecki, J. Wojtas, Bioanalysis **5**, 2287 (2013)
7. L. Menzel, A.A. Kosterev, R.F. Curl, F.K. Tittel, C. Gmachl, F. Capasso, D.L. Sivco, J.N. Baillargeon, A.L. Hutchinson, A.Y. Cho, W. Urban, Appl. Phys. B **72**, 859 (2001)
8. T. Stacewicz, J. Wojtas, Z. Bielecki, M. Nowakowski, J. Mikołajczyk, R. Mędrzycki, B. Rutecka, Opt. Electron. Rev. **20**, 34 (2012)
9. F.K. Tittel, D. Richter, A. Fried, in *Solid-State Mid-Infrared Laser Sources*, vol. 89, ed. by I.T. Sorokina, K.L. Vodopyanov (Springer, Berlin, 2003), pp. 445–516
10. Photonics Spectrum Reference Chart, Commercial Lasers Lines. Available to order: https://e.laurin.com/Default.aspx
11. J. Barria, S. Roux, J. Dherbecourt, M. Raybaut, J. Melkonian, A. Godard, M. Lefebvre, Opt. Lett. **38**, 2165 (2013)
12. B. Hardy, A. Berrou, S. Guilbaud, M. Raybaut, A. Godard, M. Lefebvre, Opt. Lett. **36**, 678 (2011)
13. J. Faist, F. Capasso, D.L. Sivco, C. Sirtori, A.L. Hutchinson, A.Y. Cho, Science **264**, 553 (1994). doi:10.1126/science.264.5158.553
14. R.F. Curl, F. Capasso, C. Gmachl, A.A. Kosterev, B. McManus, R. Lewicki, M. Pusharsky, G. Wysocki, F.K. Tittel, Chem. Phys. Lett. **487**, 1 (2010)

15. R. Engeln, G. Berden, R. Peeters, G. Meijer, Rev. Sci. Instrum. **69**, 3763 (1998)
16. J.B. Paul, L. Lapson, J.G. Anderson, App. Opt. **40**, 4904 (2001)
17. A. Rogalski, Z. Bielecki, in *Handbook of Optoelectronics*, ed. by J. Dakin, R. Brown (Taylor & Francis, New York, 2006), pp. 73–117
18. J. Wojtas, Z. Bielecki, Opto Electron. Rev. **16**, 44 (2008)
19. Photonic Devices, Electron Tube Devices and Applied Products, 2012. http://sales.hamamatsu.com/assets/pdf/catsandguides/p-dev_2012_TOTH0020E02.pdf
20. A. Rogalski, Opto Electron. Rev. **20**, 279 (2012)
21. A. Piotrowski, P. Madejczyk, W. Gawron, K. Klos, M. Romanis, M. Grudzien, A. Rogalski, J. Piotrowski, Opto Electron. Rev. **12**, 453 (2004)
22. J. Wojtas, J. Mikolajczyk, Z. Bielecki, Sensors **13**, 7570 (2013). doi:10.3390/s130607570
23. V.L. Kasyutich, I.R.K. Raj, P.A. Martin, Infrared Phys. Technol. **53**, 381 (2010)
24. P.Q. Liu, X. Wang, C.F. Gmachl, Appl. Phys. Lett. **101**, 161115 (2012). doi:10.1063/1.4761247
25. C. Gmachl, D.L. Sivco, R. Colombelli, F. Capasso, A.Y. Cho, Nature **415**, 883 (2002)
26. Z. Bozoki, A. Mohacsi, G. Szabo, Z. Bor, M. Erdelyi, W. Chen, F.K. Tittel, Appl. Spectrosc. **56**, 715 (2002)
27. A.A. Kosterev, Y.A. Bakhirkin, R.F. Curl, F.K. Tittel, Opt. Lett. **27**, 1902 (2002)
28. F.K. Tittel, L. Dong, R. Lewicki, G. Lee, A. Peralta, V. Spagnolo, Proc. SPIE **8268**, 82680F–1 (2012). doi:10.1117/12.905621
29. L. Dong, J. Wright, B. Peters, B.A. Ferguson, F.K. Tittel, S. McWhorter, Appl. Phys. B **107**, 459 (2012). doi:10.1007/s00340-012-4908-x
30. K. Namjou, S. Cai, E.A. Whittaker, J. Faist, C. Gmachl, F. Capasso, D.L. Sivco, A.Y. Cho, Opt. Lett. **23**, 219 (1998)
31. E. Normand, M. McCulloch, G. Duxbury, N. Langford, Opt. Lett. **28**, 16 (2003)